Title

White matter damage in frontotemporal dementia and Alzheimer's disease measured by diffusion MRI

Journal

Brain, 132(9)

ISSN

0006-8950

Authors

Zhang, Yu
Schuff, Norbert
Du, An-Tao
et al.

Publication Date

2009-09-01

DOI

10.1093/brain/awp071

Peer reviewed

doi:10.1093/brain/awp071 Brain 2009: 132; 2579–2592 | 2579

BRAIN
A JOURNAL OF NEUROLOGY

White matter damage in frontotemporal dementia and Alzheimer's disease measured by diffusion MRI

Yu Zhang,[1,2] Norbert Schuff,[1,2] An-Tao Du,[1] Howard J. Rosen,[3] Joel H. Kramer,[3] Maria Luisa Gorno-Tempini,[3] Bruce L. Miller[3] and Michael W. Weiner[1,2,3]

1 Center for Imaging of Neurodegenerative Diseases, Department of Veterans Affairs Medical Center, San Francisco, CA, USA
2 Department of Radiology, University of California, San Francisco, CA, USA
3 Department of Neurology, University of California, San Francisco, CA, USA

Correspondence to: Yu Zhang,
Center for Imaging of Neurodegenerative Diseases,
VA Medical Center,
4150, Clement Street,
San Francisco, CA 94121, USA.
E-mail: Yu.Zhang@ucsf.edu

Frontotemporal dementia (FTD) and Alzheimer's disease are sometimes difficult to differentiate clinically because of overlapping symptoms. Using diffusion tensor imaging (DTI) measurements of fractional anisotropy (FA) can be useful in distinguishing the different patterns of white matter degradation between the two dementias. In this study, we performed MRI scans in a 4 Tesla MRI machine including T_1-weighted structural images and diffusion tensor images in 18 patients with FTD, 18 patients with Alzheimer's disease and 19 cognitively normal (CN) controls. FA was measured selectively in specific fibre tracts (including corpus callosum, cingulum, uncinate and corticospinal tracts) as well as globally in a voxel-by-voxel analysis. Patients with FTD were associated with reductions of FA in frontal and temporal regions including the anterior corpus callosum ($P < 0.001$), bilateral anterior (left $P < 0.001$; right $P = 0.005$), descending (left $P < 0.001$; right $P = 0.003$) cingulum tracts, and uncinate tracts (left $P < 0.001$; right $P = 0.005$), compared to controls. Patients with Alzheimer's disease were associated with reductions of FA in parietal, temporal and frontal regions including the left anterior ($P = 0.003$) and posterior ($P = 0.002$) cingulum tracts, bilateral descending cingulum tracts ($P < 0.001$) and left uncinate tracts ($P < 0.001$) compared to controls. When compared with Alzheimer's disease, FTD was associated with greater reductions of FA in frontal brain regions, whereas no region in Alzheimer's disease showed greater reductions of FA when compared to FTD. In conclusion, the regional patterns of anisotropy reduction in FTD and Alzheimer's disease compared to controls suggest a characteristic distribution of white matter degradation in each disease. Moreover, the white matter degradation seems to be more prominent in FTD than in Alzheimer's disease. Taken together, the results suggest that white matter degradation measured with DTI may improve the diagnostic differentiation between FTD and Alzheimer's disease.

Keywords: Alzheimer's disease; frontotemporal dementia; diffusion tensor imaging; diffusion tensor fibre tracking

Abbreviations: CN = cognitively normal; D_{ax} = axial diffusivity; D_{ra} = radial diffusivity; DTI = diffusion tensor imaging; FA = fractional anisotropy; FDR = false discovery rate; FTD = frontotemporal dementia; ICC = intraclass correlation coefficients; MMSE = Mini-Mental State Examination; ROI = regions of interest; TOI = tracts of interest; WMSH = white matter signal hyperintensities

Received October 1, 2008. Revised February 13, 2009. Accepted February 18, 2009. Advance Access publication May 12, 2009

Introduction

Frontotemporal dementia (FTD), the behavioural variant of frontotemporal lobar degeneration, is sometimes difficult to clinically differentiate from Alzheimer's disease, due to overlapping clinical symptoms (McKhann *et al*., 1984; Neary *et al*., 1998; Siri *et al*., 2001). Structural (Kitagaki *et al*., 1998; Laakso *et al*., 2000; Rosen *et al*., 2002; Gee *et al*., 2003) and functional (Johnson *et al*., 1987; Miller *et al*., 1991; Julin *et al*., 1995; Bartenstein *et al*., 1997; Pickut *et al*., 1997; Ishii *et al*., 1998; Charpentier *et al*., 2000; Varma *et al*., 2002; Varrone *et al*., 2002; Diehl *et al*., 2004; Grimmer *et al*., 2004; Kim *et al*., 2005; McMurtray *et al*., 2006) neuroimaging studies have shown characteristic differences of grey matter abnormalities in FTD and Alzheimer's disease. In FTD, MRI studies reported regional patterns of grey matter atrophy in primarily frontal lobe regions (Rosen *et al*., 2002; Perry *et al*., 2006; Whitwell *et al*., 2006), similar to the regional patterns of functional changes measured by reduced cerebral blood flow and glucose metabolism from SPECT and PET studies, respectively (Jeong *et al*., 2005; Coulthard *et al*., 2006; Diehl-Schmid *et al*., 2007). By comparison, brain atrophy in Alzheimer's disease is initially observed in medial temporal lobe regions, whereas functional changes are more prominent in the parietal lobe (including the posterior cingulate gyrus and lateral parietotemporal areas). The frontal lobe regions are generally spared in Alzheimer's disease until late stages (see review papers: Anderson *et al*., 2005; Drzezga, 2008; Ries *et al*., 2008). New MRI findings have shown that both FTD (Cardenas, *et al*., 2007; Chao *et al*., 2007) and Alzheimer's disease (Double *et al*., 1996; Teipel *et al*., 2002) can involve white matter loss. However, the regional distribution of loss is difficult to study due to lack of discernable anatomical features of white matter in conventional MRI.

Diffusion tensor imaging (DTI) has become the method of choice for detecting white matter alterations in the human brain (Le Bihan *et al*., 2001). DTI, which is sensitive to water diffusion, captures microstructural alterations of tissue by measuring systematic directional changes in water diffusivity. The directionality of diffusion is usually expressed as fractional anisotropy (FA), which ranges from zero for isotropic diffusion to unity for diffusion exclusively along one direction (Pierpaoli and Basser, 1996). For example, well-organized (i.e. strongly myelinated) white matter tracts have high-FA values because water diffuses more freely in the direction of the axonal fibre tracts, while diffusion perpendicular to the fibres is relatively restricted. As the fibres degenerate, diffusion becomes less directional and thus the value of FA decreases. DTI has been used to study normal aging and a variety of neurological diseases (Ellis *et al*., 1999; Yoshikawa *et al*., 2004; Aoki *et al*., 2005; Shiga *et al*., 2005) including Alzheimer's disease and FTD. In Alzheimer's disease, DTI studies reported FA reductions in a variety of white matter regions including the posterior corpus callosum, posterior cingulum, fornix and bilaterally in the uncinate fibres using regions of interest (ROI) analyses (Rose *et al*., 2000; Bozzali *et al*., 2002; Takahashi *et al*., 2002; Fellgiebel *et al*., 2004, 2005; Head *et al*., 2004; Sugihara *et al*., 2004; Choi *et al*., 2005; Naggara *et al*., 2006; Taoka *et al*., 2006; Huang *et al*., 2007; Ringman *et al*., 2007; Stahl *et al*., 2007; Zhang *et al*., 2007; Yasmin *et al*., 2008). Other regionally unbiased DTI studies of Alzheimer's disease using voxel-by-voxel analyses, have shown FA reductions in parietal and temporal lobe regions as well as in the thalamus and internal capsule (Medina *et al*., 2006; Xie *et al*., 2006; Teipel *et al*., 2007; Rose *et al*., 2008). To this date, few DTI studies of FTD have reported white matter damage. One study found FA changes in the superior and the inferior longitudinal fasciculus (Borroni *et al*., 2007) using a regionally unbiased analysis. Another study found FA changes additionally in the uncinate fibres and the genu of the corpus callosum using ROI analysis (Matsuo *et al*., 2008). Although these findings imply that the distribution of white matter damage is different between FTD and Alzheimer's disease, no DTI study to our knowledge has directly compared DTI findings in FTD with those in Alzheimer's disease. Furthermore, comparisons of previous results are complicated by the fact that some DTI studies used voxel-by-voxel tests (Medina *et al*., 2006; Xie *et al*., 2006; Borroni *et al*., 2007; Teipel *et al*., 2007; Rose *et al*., 2008) whereas others limited regional analyses to an *a priori* defined ROI, which was often guided by fibre tracts (Taoka *et al*., 2006; Matsuo *et al*., 2008; Yasmin *et al*., 2008). Although ROI can provide anatomically reliable information, especially when combined with tractography to guide the ROI, the approach requires *a priori* hypotheses about regional distributions of alterations. In contrast, voxel-wise analyses circumvent the regional bias but are problematic with respect to the accurate alignment of tract anatomy. Using both approaches together may provide complementary information.

We employed both voxel-wise and tractography-guided ROI tests in this study to compare white matter alterations in FTD and Alzheimer's disease. Our main objectives were: (i) to determine if FTD is associated with a characteristic regional pattern of FA reduction—implying systematic white matter degradation—in comparison to healthy elderly subjects; (ii) to replicate previous findings of regional FA reductions in Alzheimer's disease; and (iii) to compare the regional patterns of FA reductions in FTD to that of Alzheimer's disease.

Subjects and Methods

Subjects

Eighteen FTD patients (mean age and standard deviation: 62.1 ± 10.7 years) with a Mini-Mental State Examination (MMSE) (Folstein *et al*., 1975) score of on average 24.1 ± 4.7, 18 patients with Alzheimer's disease (age: 62.8 ± 7.1 years; MMSE: 21.7 ± 5.8) and 19 cognitive normal (CN) subjects (age: 61.5 ± 10.6 years; MMSE: 29.5 ± 0.5) were included in this cross-sectional MRI study. A summary of the subject demographics and relevant clinical information is listed in Table 1. The patients with FTD and Alzheimer's disease were recruited from the Memory and Aging Centre of the University of California, San Francisco. All patients were diagnosed based upon information obtained from an extensive clinical history and physical examination. The MR images were used to rule out other major neuropathologies such as tumours, strokes, severe white matter disease or inflammation but not to diagnose dementia. The subjects were between 30- and 80-years old and without history of brain trauma, brain tumour,

Table 1 Demographic and clinical summary

	Cognitive normal	Frontotemporal dementia	Alzheimer's disease
Number of DTI	19	18	18
Age (years)	61.5 ± 10.6	62.1 ± 10.7	62.8 ± 7.1
Age range (years)	33–73	32–77	51–74
Sex (M:F)	11:8	12:6	11:7
MMSE*	29.5 ± 0.5	24.1 ± 4.7	21.7 ± 5.8
WMSH (severe:moderate: mild)	3:2:14	3:2:13	1:2:15

*MMSE scores in FTD and Alzheimer's disease were significant lower than in CN ($P < 0.001$), but not significantly different between FTD and Alzheimer's disease.

stroke, epilepsy, alcoholism, psychiatric illness and other systemic diseases that affect brain function. FTD was diagnosed according to the consensus criteria established by Neary *et al*. (1998). All FTD patients were diagnosed with the frontal variant subtype, two of which had concurrent motor neuron-related symptoms. Patients with Alzheimer's disease were diagnosed according to the criteria of the National Institute of Neurological and Communicative Disorders and Stroke-Alzheimer's Disease and Related Disorders Association (NINCDS/ADRDA) (McKhann *et al*., 1984). All subjects received a standard battery of neuropsychological tests including assessment of global cognitive impairment by the MMSE score and global functional impairment by the Clinical Dementia Rating (CDR) scale (Morris, 1993). The neuropsychological tests were not used for clinical diagnosis but rather to characterize the cognitive deficits of the patients, although a cognitive pattern of impaired executive functioning with relatively well preserved memory and spatial ability was considered a supportive feature of FTD. An experienced radiologist reviewed the severity of white matter signal hyperintensities (WMSH) on MRI. The severity of WMSH was classified as mild (score 1), moderate (score 2) or severe (score >3), according to the Schelten's rating scale (Scheltens *et al*., 1993). All subjects or their guardians gave written informed consent before participating in the study, which was approved by the Committees of Human Research at the University of California at San Francisco.

Data acquisition and processing

DTI was performed on a 4 Tesla (Bruker/Siemens) MRI system, equipped with a birdcage transmit and eight channel receive coil. DTI was based on a dual spin-echo echo-planar imaging (EPI) sequence supplemented with parallel imaging acceleration (GRAPPA) (Griswold *et al*., 2002) with a factor 2 to reduce susceptibility distortions. Other imaging parameters were: TR/TE = 6000/77 ms; field of view 256 × 224 cm; 128 × 112 matrix size, yielding 2 × 2 mm^2 in-plane resolution; 40 continuous 3 mm slices. A reference image (no diffusion gradient b = 0) and six diffusion-weighted images ($b = 800$ s/mm^2 along six non-collinear directions) were acquired. Four DTI scans were acquired and averaged after motion correction to boost signal-to-noise. The total acquisition time of DTI was 4 min. Test–retest studies showed that measurement reproducibility of the DTI protocol yielded intraclass correlation coefficients (ICC) of 0.8 and higher in the vast majority of brain regions.

Maps of FA and mean diffusivity were computed using Volume-one and dTV software (The software dTV is available via following http://www.ut-radiology.umin.jp/people/masutani/dTV.htm) (Masutani *et al*., 2003). In addition, axial diffusivity (D_{ax}), which is equivalent to the magnitude of the largest eigenvalues of the tensor (λ_1) and radial diffusivity (D_{ra}), which is the average of the other two eigenvalues [($\lambda_2 + \lambda_3$)/2] were also calculated, supplementing the analysis of FA. Image co-registration and spatial normalization for voxel-wise statistical evaluations was conducted using SPM2 software (http://www.fil.ion.ucl.ac.uk/spm).

Tracts of interest measurements

Fibre tracking was performed with the Volume-one and dTV software packages, which are based on the fibre assignment by continuous tracking (FACT) approach (Mori *et al*., 1999) to achieve a three-dimensional tract reconstruction. The identification of fibres tracts was initiated by placing a 'Seed' and a 'Target' area in anatomical regions through which the particular fibres are expected to propagate as described by Wakana *et al*. (2004). The propagation of tracts was constrained by a lower threshold of FA = 0.18 and limits of angular deviations from the path trajectory of <45°. Trajectories that passed through the Seed and Target were assigned to specific fibre tracts based on anatomical knowledge. Several major fibre pathways were selected due to their relations to higher brain functions. The tracts included: (i) the cingulum tract, which is associated with memory function, connects the anterior and posterior cingulate gyrus and descends into the medial temporal lobe; (ii) the uncinate fascicules, which is associated with memory and behavioural functions, connects the inferior frontal lobe with the anterior medial temporal lobe; (iii) the corpus callosum, which is associated with various functions depending on the location along the corpus callosum, connects the brain hemispheres; and (iv) the corticospinal tract, which is associated with movement control, connects the primary motor cortex to the spinal cord. Figure 1 depicts the placements of the Seed and Target area for tracking these fibres:

(i) Fibre tracking of the corpus callosum was performed by placing the Seed on the mid-sagittal slice along the full length of the corpus callosum (Fig. 1C);
(ii) Tracking of the cingulum fibres, which are shorter and more curved than the corpus callosum, was performed separately for the upper and descending portions of these fibres by using two pairs of Seeds and Targets for each portion. One pair was placed at the anterior and posterior terminal of the cingulate regions. The other pair was placed at the lower and higher ends of the parahippocampus (Fig. 1B);
(iii) Tracking of the uncinate fibres was performed by placing the Seed and Target on a coronal slice adjacent to the most anterior point of the frontal and temporal terminal of the uncinate tract (Fig. 1D);
(iv) Tracking of the corticospinal tract was performed by placing the Seed on the cerebral peduncle and the Target on the superior precentral gyrus and adjacent white matter (Fig. 1A).

The reconstruction of the selected fibres is illustrated in Fig. 2. The fibre tracts were then transformed into binary maps to guide tracts of interest (TOI) measurements. The TOIs were further divided into several portions according to anatomical location. For example, the TOIs of the callosal fibre tracts were divided into an anterior and a posterior portion of the corpus callosum, such that the anterior corpus callosum included mainly fibres connecting to the frontal lobe and the

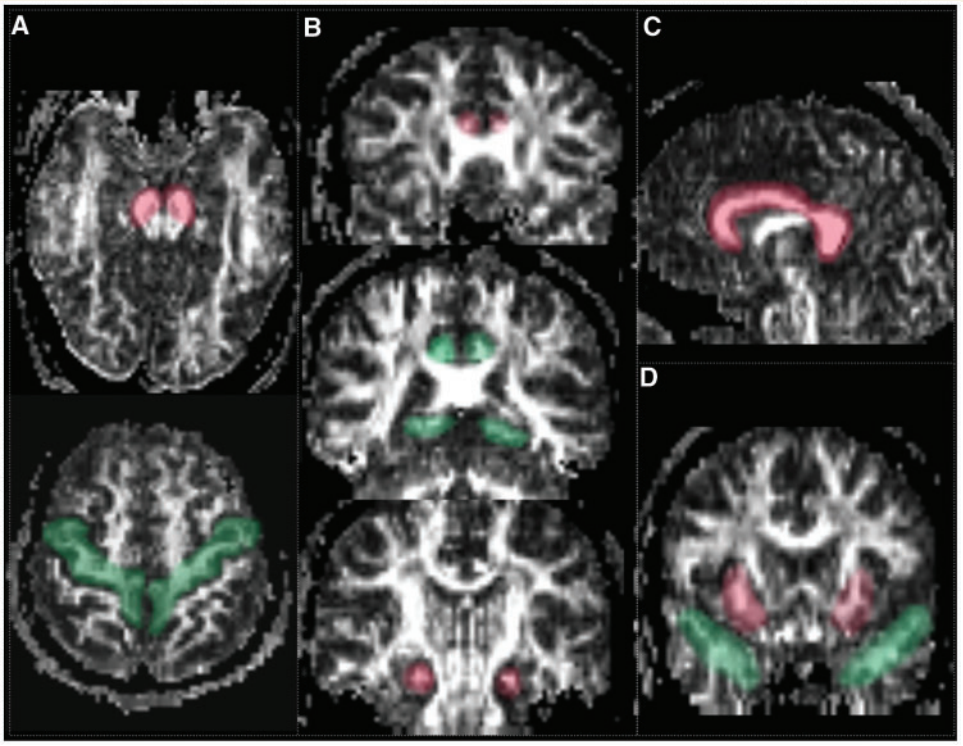

Figure 1 Placement of Seeds and Targets for TOI analysis: (**A**) To define the corticospinal tract, the Seed (red colour) was drawn on axial slice on the cerebral peduncle at the level of the decussation of the superior cerebellar peduncle; the Target (green colour) was placed on an axial slice on the precentral gyrus (primary motor cortex), anterior to the central sulcus. (**B**) To define the upper part of cingulum fibres, Seed (red) and Target (green) were placed on the anterior and posterior cingulum areas on the same coronal slice level as the genu and splenium of the corpus collosum, respectively. To define the descending part of cingulum, the Seed (red) and Target (green) were placed as shown in the figure. (**C**) The definition of the callosal fibre required only a single Seed (red) on a mid-sagittal slice. (**D**) To define the uncinate fascicules, the Seed (red) and Target (green) were positioned on a coronal slice on the most posterior slice where the frontal and temporal lobes appear separated.

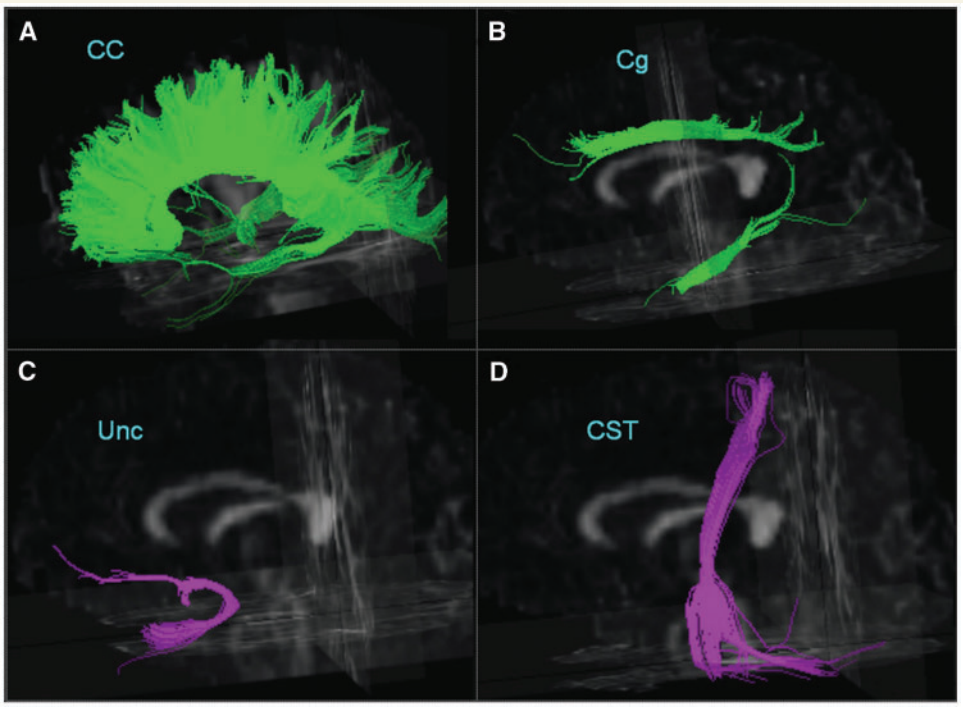

Figure 2 Illustration of fibre tracts of the corpus callosum (CC), cingulum (Cg), uncinate (Unc) and the corticospinal tract (CST) from a single subject superimposed on a 3-dimensional FA image.

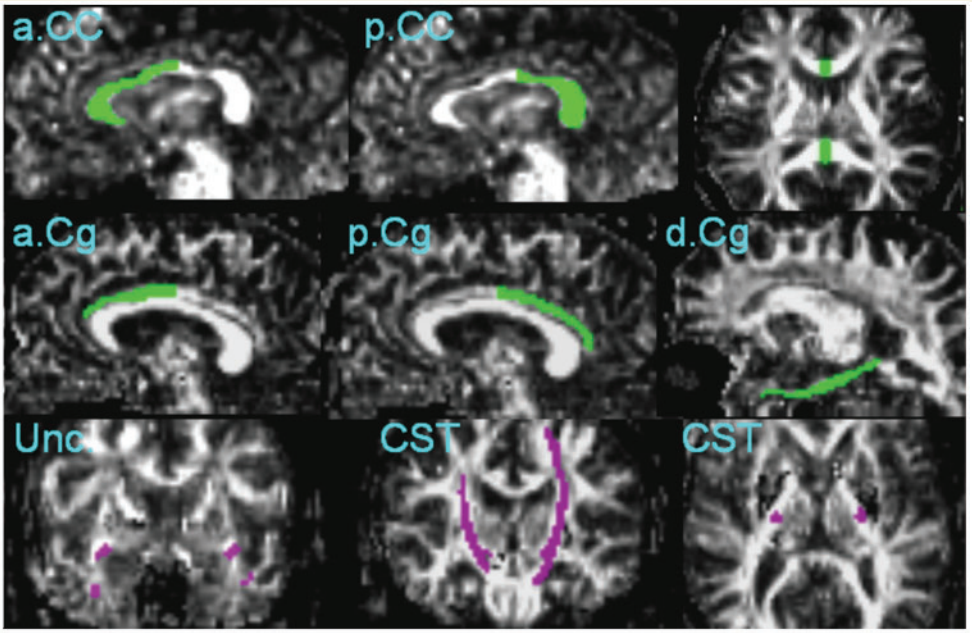

Figure 3 Illustration of location and coverage of TOI: anterior corpus callosum (a.CC), posterior corpus callosum (p.CC), anterior cingulum (a.Cg), posterior cingulum (p.Cg), descending cingulum (d.Cg), uncinate tracts (Unc) and corticospinal tracts (CST).

posterior corpus callosum included fibres connecting to the parietal and temporal lobes. Similarly, the cingulum fibre tracts were divided into three portions. The upper cingulum tract was separated into two: (i) an anterior portion and (ii) a posterior portion, containing mainly fibres that connect to the anterior and posterior cingulate gyri, respectively, while (iii) the third portion consisting of the descending cingulum, which include mainly fibres passing through the parahippocampus and the bottom of the temporal lobe. In total, six TOI pairs were selected as illustrated in Fig. 3. For each TOI, the mean FA value as well as mean D_{ax} and mean D_{ra} were computed for further analysis.

An experienced radiologist (Y.Z.), blinded to diagnosis, performed the placements of the Seeds and Targets for tractography. To determine the reproducibility of tractography, the same rater performed tractography twice, 2 months apart, on 12 randomly selected subjects. Reproducibility was based on fibre counts and expressed as ICC. An ICC of 0.99 was achieved for the callosal fibre tracking, 0.93 for the cingulum, 0.95 for the uncinate and 0.96 for the corticospinal tract tractography.

For the group analysis, we first determined whether diagnosis had a global effect on FA (or D_{ra}, D_{ax}) by multivariate analysis of variance (MANOVA) that simultaneously included all TOIs. This was followed by univariate *post hoc* tests of each TOI to determine local effects. Age and gender were added as covariates. To account for multiple comparisons the significance level was set to $\alpha = 0.01$ for these tests.

Voxel-wise measurements

We also tested local effects on a voxel-by-voxel basis without constraints to the TOIs. For this approach, a study specific FA template was created for the spatial normalization of the DTI data using SPM2. First, each subject's diffusion reference image (b0 image), which generally provides sufficient anatomical features, was transformed into the EPI-derived MNI (Montreal Neurological Institute) template in SPM by iterative non-linear transformations, yielding a mean b0-image of the population. The same transformation parameters were then applied to the corresponding FA maps to obtain a customized mean FA image of the study population. Second, the FA map of each subject was non-linearly transformed again, for spatial normalization but this time to the customized FA template of the population that was created in step one. To reduce effects of local mis-registrations, the spatially normalized FA maps were smoothed using an isotropic Gaussian kernel with a full width at half height maximum of 4 mm. Group comparisons were performed voxel-wise by regressing the local FA intensity against diagnosis with adjustments for age and sex. The concept of false discovery rate (FDR) was used to control for multiple comparisons at a significance level of $\alpha = 0.05$ (Genovese *et al.*, 2002). The voxel-wise analysis was considered exploratory since image mis-registrations from spatial normalization can mimic FA alterations especially, if brain atrophy is present. We sought to control for effects from mis-registrations first by using FA = 0.15 as lower threshold to avoid voxels in primarily CSF or grey matter regions and second by using only voxels that all subjects had in common. Similarly to FA, D_{ra} and D_{ax} images were also analysed voxel-by-voxel. Although, these rules may not exclude all artefacts from mis-registrations, the supplementary analysis based on TOI should lend support to regionally unbiased findings.

Results

Demographics

Table 1 lists the demographics and clinical data of the subjects. The groups did not differ by age ($P > 0.6$, ANOVA) or gender distribution ($P > 0.8$, Chi-square). As expected, patients with FTD and Alzheimer's disease scored significantly lower than CN

Table 2 Group differences from TOI analysis of regional FA values as a function of diagnosis; the synopsis of the findings from the voxel-wise analysis

Region	TOI analysis								
	FA (mean ± SD)			*P*-values			Voxel-wise analysis		
	CN	FTD	AD	FTD<CN	AD<CN	FTD<AD[a]	FTD<CN	AD<CN	FTD<AD[b]
a.CC	0.54 ± 0.03	0.46 ± 0.06	0.51 ± 0.04	0.0002	NS	0.007	S	NS	S
p.CC	0.64 ± 0.04	0.61 ± 0.04	0.61 ± 0.04	NS	0.02	NS	S	S	NS
L.a.Cg	0.50 ± 0.04	0.43 ± 0.05	0.45 ± 0.05	<0.0001	0.003	NS	S	NS	S
R.a.Cg	0.41 ± 0.03	0.37 ± 0.04	0.39 ± 0.05	0.005	NS	NS	S	NS	S
L.p.Cg	0.48 ± 0.04	0.45 ± 0.04	0.44 ± 0.03	NS	0.002	NS	S	S	NS
R.p.Cg	0.43 ± 0.04	0.41 ± 0.04	0.41 ± 0.03	NS	NS	NS	S	NS	NS
L.d.Cg	0.36 ± 0.02	0.32 ± 0.03	0.32 ± 0.03	<0.0001	<0.0001	NS	S	S	NS
R.d.Cg	0.39 ± 0.03	0.35 ± 0.05	0.34 ± 0.04	0.003	0.0001	NS	S	NS	NS
L.Unc	0.39 ± 0.03	0.34 ± 0.03	0.36 ± 0.03	<0.0001	0.0004	0.04	S	S	S
R.Unc	0.38 ± 0.04	0.33 ± 0.05	0.36 ± 0.04	0.005	NS	0.03	S	S	S
L.CST	0.52 ± 0.03	0.52±0.03	0.53 ± 0.03	NS	NS	NS	NS	NS	NS
R.CST	0.58 ± 0.02	0.57 ± 0.04	0.58 ± 0.03	NS	NS	NS	NS	NS	NS

a No region showed significant lower FA in Alzheimer's disease when compared to FTD (AD<FTD).
b No region showed significant lower FA in Alzheimer's disease when compared to FTD (AD<FTD).
a.CC/p.CC = anterior/posterior corpus callosum; L.a.Cg/R.a.Cg = Left/Right anterior cingulum; L.p.Cg/R.p.Cg = Left/Right posterior cingulum; L.d.Cg/R.d.Cg = Left/Right descending cingulum; L.Unc/R.Unc = Left/Right uncinate fasciculus; L.CST/R.CST = Left/Right corticospinal tract.

Table 3 Group differences from TOI analysis of regional radial diffusivity (D_{ra}) values as a function of diagnosis; the synopsis of the findings from voxel-wise analysis

Region	TOI analysis								
	D_{ra} (mean ± SD)			*P*-values			Voxel-wise analysis		
	CN	FTD	AD	FTD>CN	AD>CN	FTD>AD[a]	FTD>CN	AD>CN	FTD>AD[b]
a.CC	0.70 ± 0.09	0.93 ± 0.21	0.77 ± 0.10	0.0002	0.03	0.01	S	S	S
p.CC	0.57 ± 0.06	0.64 ± 0.10	0.65 ± 0.09	0.01	0.004	NS	S	S	NS
L.a.Cg	0.55 ± 0.05	0.67 ± 0.07	0.61 ± 0.07	<0.0001	0.004	0.02	S	S	S
R.a.Cg	0.61 ± 0.04	0.70 ± 0.06	0.65± 0.08	<0.0001	NS	0.03	S	S	S
L.p.Cg	0.55 ± 0.05	0.59 ± 0.05	0.60 ± 0.05	0.008	0.002	NS	S	S	NS
R.p.Cg	0.56 ± 0.04	0.61 ± 0.05	0.60 ± 0.05	0.01	0.003	NS	S	S	NS
L.d.Cg	0.66 ± 0.06	0.81 ± 0.15	0.81 ± 0.12	0.001	<0.0001	NS	S	S	S
R.d.Cg	0.62 ± 0.06	0.74 ± 0.14	0.78 ± 0.16	0.003	0.0003	NS	S	S	NS
L.Unc	0.69 ± 0.04	0.84 ± 0.12	0.77 ± 0.07	<0.0001	<0.0001	0.01	S	S	S
R.Unc	0.68 ± 0.06	0.89 ± 0.21	0.75 ± 0.09	<0.0001	0.01	0.002	S	S	S
L.CST	0.61 ±0.05	0.63 ± 0.07	0.60 ± 0.07	NS	NS	NS	NS	NS	NS
R.CST	0.49 ± 0.03	0.54 ± 0.09	0.49 ± 0.04	0.01	NS	0.02	S	NS	S

a No region showed significant increased D_{ra} in Alzheimer's disease when compared to FTD (AD>FTD).
b No region showed significant increased D_{ra} in Alzheimer's disease when compared to FTD (AD>FTD).
a.CC/p.CC = anterior/posterior corpus callosum; L.a.Cg/R.a.Cg = Left/Right anterior cingulum; L.p.Cg/R.p.Cg = Left/Right posterior cingulum; L.d.Cg/R.d.Cg = Left/Right descending cingulum; L.Unc/R.Unc = Left/Right uncinate fasciculus; L.CST/R.CST = Left/Right corticospinal tract.

subjects on MMSE ($P < 0.001$, ANOVA). Differences in MMSE scores between patients with FTD and Alzheimer's disease were not significant ($P = 0.16$), irrespective of age. WMSH severity, which is subdivided into mild, severe and moderate groups, were similar between the groups ($P = 0.7$).

TOI analysis

Group differences of regional FA values as a function of diagnosis are summarized in Table 2. This was performed separately for each TOI region and the corresponding results of D_{ax} and D_{ra} are summarized in Tables 3 and 4. The results from the voxel-wise analysis are also listed in the tables for comparison.

Compared to CN, patients with FTD had lower FA values in the anterior corpus callosum ($P < 0.001$), bilateral anterior cingulum (left $P < 0.001$; right $P = 0.005$), bilateral descending cingulum (left $P < 0.001$; right $P = 0.003$), and uncinate fibres (left $P < 0.001$; right $P = 0.005$). In most regions, the FA reductions correspond to an increase of D_{ra} and in some regions to an increase of D_{ax} as well. In particular, the increase of D_{ra} between FTD and

Table 4 Group differences from TOI analysis of regional axial diffusivity (D_{ax}) values as a function of diagnosis; the synopsis of the findings from voxel-wise analysis

Region	TOI analysis								
	D_{ax} (mean ± SD)			*P*-values			Voxel-wise analysis		
	CN	FTD	AD	FTD>CN	AD>CN	FTD>AD[a]	FTD>CN	AD>CN	FTD>AD[b]
a.CC	1.87 ± 0.12	2.09 ± 0.18	1.97 ± 0.09	<0.0001	0.007	0.02	S	S	S
p.CC	1.85 ± 0.10	1.91 ± 0.10	1.93 ± 0.10	0.04	0.02	NS	NS	S	NS
L.a.Cg	1.44 ± 0.07	1.45 ± 0.08	1.43 ± 0.07	NS	NS	NS	S	NS	NS
R.a.Cg	1.28 ± 0.05	1.34 ± 0.09	1.31 ± 0.06	0.03	NS	NS	S	NS	NS
L.p.Cg	1.31 ± 0.06	1.33 ± 0.06	1.32 ± 0.08	NS	NS	NS	NS	NS	NS
R.p.Cg	1.22 ± 0.04	1.24 ± 0.06	1.24 ± 0.07	NS	NS	NS	NS	NS	NS
L.d.Cg	1.25 ± 0.07	1.37 ± 0.16	1.37 ± 0.13	0.008	0.001	NS	S	S	NS
R.d.Cg	1.21 ± 0.07	1.31 ± 0.17	1.34 ± 0.18	0.04	0.004	NS	S	S	NS
L.Unc	1.31 ± 0.08	1.43 ± 0.13	1.38 ± 0.08	0.001	0.02	NS	S	S	NS
R.Unc	1.29 ± 0.06	1.51 ± 0.19	1.34 ± 0.06	<0.0001	0.03	0.0002	S	S	NS
L.CST	1.43 ± 0.06	1.48 ± 0.08	1.45 ± 0.07	NS	NS	NS	S	NS	NS
R.CST	1.35 ± 0.05	1.39 ± 0.06	1.36 ± 0.04	NS	NS	NS	S	NS	NS

a No region showed significant increased D_{ax} in Alzheimer's disease when compared to FTD (AD>FTD).
b No region showed significant increased D_{ax} in Alzheimer's disease when compared to FTD (AD>FTD).
a.CC/p.CC = anterior/posterior corpus callosum; L.a.Cg/R.a.Cg = Left/Right anterior cingulum; L.p.Cg/R.p.Cg = Left/Right posterior cingulum; L.d.Cg/R.d.Cg = Left/Right descending cingulum; L.Unc/R.Unc = Left/Right uncinate fasciculus; L.CST/R.CST = Left/Right corticospinal tract.

CN expanded to the posterior cingulum, where no significant difference was observed when using FA.

Patients with Alzheimer's disease when compared to CN had lower FA values in the left posterior cingulum ($P = 0.002$), left anterior cingulum ($P = 0.003$), bilateral descending cingulum (both $P < 0.001$) and left uncinate ($P < 0.001$) fibres, which was similar to FTD. The posterior corpus callosum showed a trend ($P = 0.02$) towards lower FA values in Alzheimer's disease than in CN. In most regions, the FA reductions correspond to an increase of D_{ra} and in some regions to an increase of D_{ax}. These results were similar to those found in comparing FTD and CN. Most interestingly, Alzheimer's disease had substantially increased D_{ra} values ($P = 0.004$) in the posterior corpus callosum, in absence of significant changes in D_{ax} and FA.

Compared to Alzheimer's disease, patients with FTD had lower FA values in the anterior corpus callosum ($P = 0.007$) and also showed a trend towards lower FA values in bilateral uncinate fibres (left $P = 0.04$; right $P = 0.03$). Interestingly, the significant difference in FA between FTD and Alzheimer's disease in the anterior corpus callosum disappeared for D_{ra} and D_{ax}. On the other hand, D_{ra} and D_{ax} values in the right uncinate fibres were significantly higher in FTD than Alzheimer's disease ($P = 0.002$ and $P = 0.0002$, respectively) whereas differences in FA were not significant. Alzheimer's disease compared to FTD showed no significant reductions of FA, nor significant increases of D_{ra} and D_{ax} values.

Voxel-wise analysis

Regional FA reductions in patients with FTD and Alzheimer's disease relative to CN subjects, as well as FA differences between patients with FTD and Alzheimer's disease, are depicted in Figs 4–6. Significant FA reductions are superimposed on the FA template to better visualize the anatomical locations. For comparison, the TOI regions from the tractography-based analysis are also superimposed on the FA template. For each TOI region the corresponding findings from the voxel-wise analysis [significant (S) or not significant (NS)] are also listed in Tables 2–4.

Compared to CN, patients with FTD had widespread FA reductions bilaterally in frontal and temporal white matter. The most significant FA reductions involved the anterior corpus callosum, bilateral anterior and descending cingulum and uncinate fibres. The thalamic radiation in the anterior limb of internal capsule, bilateral superior longitudinal fascicules and part of the posterior corpus callosum were also affected. In general, the distributions of increased D_{ra} and D_{ax} values in FTD corresponded to the distribution of decreased FA value. Furthermore, D_{ra} and D_{ax} differences between FTD and CN were more widespread in bilateral frontal and temporal lobe white matter, brain stem and posterior cingulum as compared to FA differences.

Compared to CN, patients with Alzheimer's disease had FA reductions bilaterally in parietal and temporal white matter as well as in some frontal periventricular areas. Significant FA reductions included the posterior corpus callosum, left posterior cingulum, left descending cingulum and bilateral uncinate fibres. FA reductions were also detected in a small part of the anterior limb of internal capsule. Compared to FA, the distributions of D_{ra} and D_{ax} are more widespread in Alzheimer's disease, especially in parietal and temporal regions as well as in frontal periventricular regions.

Compared to Alzheimer's disease, patients with FTD had lower FA values bilaterally in frontal white matter. Involvement included inferior temporal white matter regions as well as anterior corpus callosum, bilateral anterior cingulum and uncinate fibres. Lower FA values in FTD relative to Alzheimer's disease were also detected in bilateral superior longitudinal fascicules, and the anterior limb of internal capsule. In general, the distributions of increased D_{ra} and D_{ax} values in FTD were more widespread than the distribution of reduced FA. This pattern was most prominent in frontal and

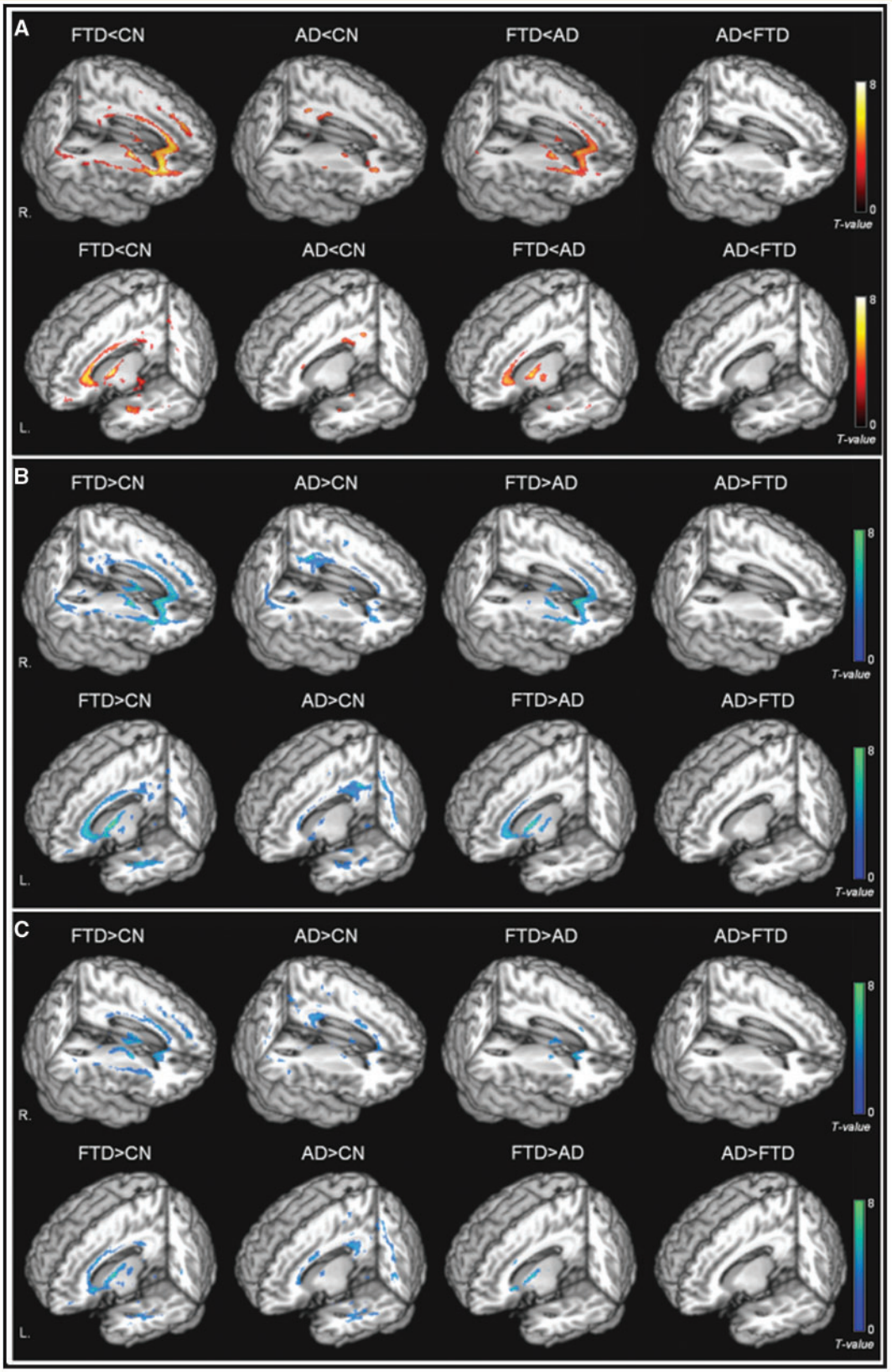

Figure 4 Rendered display of DTI changes (**A**) reduced FA (warm colours); (**B**) increased D_{ra} (cool colours); (**C**) increased D_{ax} (cool colours) in FTD or Alzheimer's disease compared with cognitively normal subjects, as well as direct comparisons between FTD and Alzheimer's disease.

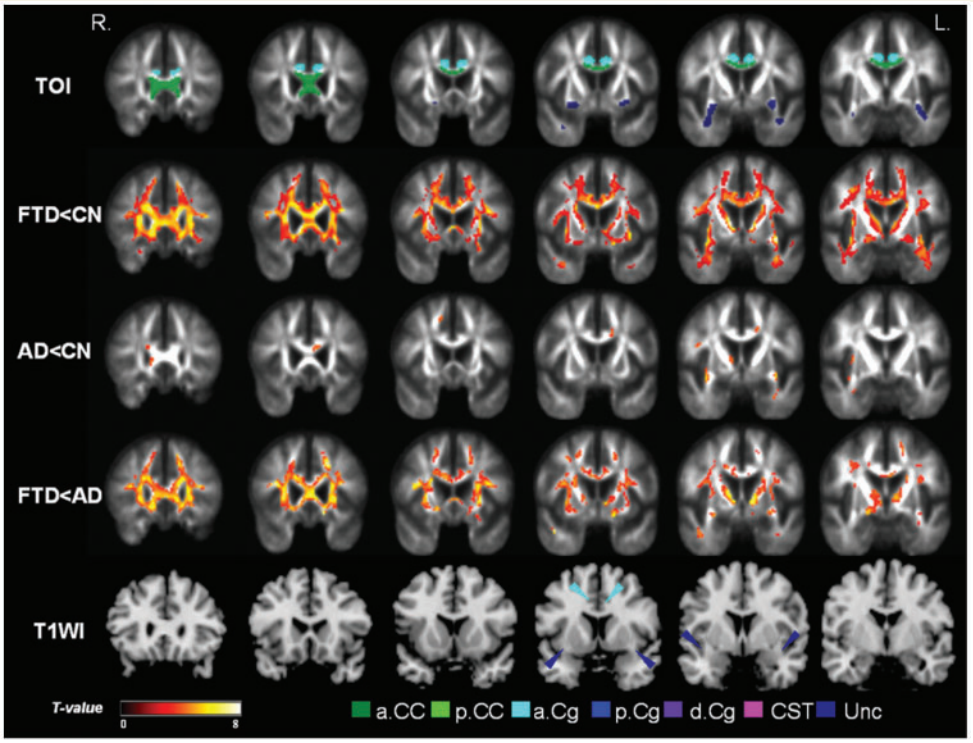

Figure 5 Coronal view of the regional FA reductions between groups in anterior brain: the top row indicates regions of the tracts of interest (TOIs) analysis for comparison with the voxel-wise analyses in the rows below. The second row (FTD<CN) shows FA reductions in FTD relative to cognitively normal involving the anterior frontal and temporal brain. The third row (AD<CN) shows the regional FA reductions in Alzheimer's disease relative to cognitively normal involving only a few regions in left anterior cingulum and bilateral uncinate fibres. The fourth row (FTD<AD) shows FA reductions in FTD relative to Alzheimer's disease indicating FTD had significantly lower FA in vast regions of bilateral frontal lobes including anterior corpus callosum, bilateral anterior cingulum, uncinate fibres and anterior limb of internal capsule. Last row (T1WI) depicts the anatomical locations on a T_1-weighted brain template. The areas with significantly decreased FA values are marked in warm colours with threshold $P_{FDR} = 0.05$.

inferior white matter regions. Patients with Alzheimer's disease compared to FTD showed no region with significantly lower FA, nor significantly higher D_{ra} and D_{ax} values.

Discussion

The main findings of this study are: (i) FTD is associated with FA reduction in the anterior corpus callosum, bilateral anterior and descending cingulum and uncinate fibre tracts. A voxel-by-voxel analysis showed even more widespread FA reduction in FTD which involved frontal and temporal white matter regions, expanded to parietal, and spared occipital white matter. (ii) In contrast, Alzheimer's disease is associated with FA reduction in bilateral descending cingulum, left posterior and anterior cingulum, and left uncinate fibre tracts, which is in agreement with previous DTI studies. (iii) A direct comparison between FTD and Alzheimer's disease reveals that FTD is associated with lower FA values than Alzheimer's disease in frontal fibres including the anterior corpus callosum, and bilateral uncinate fibres. By contrast, Alzheimer's disease shows no significant regional FA reductions relative to FTD. Furthermore, most FA reductions are related to increased D_{ra} and some to increased D_{ax} values. Taken together, the different regional patterns of DTI in FTD and Alzheimer's disease compared to CN suggest a characteristic distribution of white matter degradation for each disease. FTD is shown to be associated with more extensive white matter degradation than Alzheimer's disease.

The findings suggest that frontal and temporal white matter regions are particularly vulnerable in individuals diagnosed with FTD. These regions include: the anterior corpus callosum, which contains fibres connecting to frontal cortex; bilateral anterior and the descending cingulum, which connect to the major limbic cortices including anterior cingulate gyrus and hippocampus and bilateral uncinate fibres, which connect the frontal and inferior temporal cortices. This regional pattern of FA reduction overlaps with the pattern of white matter atrophy that we have previously reported with structural MRI studies (Cardenas, *et al*., 2007; Chao *et al*., 2007). Patterns of grey matter atrophy and hypoperfusion have also been reported in FTD (Rosen *et al*., 2002; Jeong *et al*., 2005; McMurtray *et al*., 2006; Seeley *et al*., 2008). Taken together, these findings suggest that degradation of the white matter fibre bundles occurs in association with white matter loss and cortical abnormalities in FTD. Therefore, white matter changes are a major pathological characteristic of FTD (Larsson *et al*., 2000, 2004). The DTI findings of white matter vulnerability in FTD are most likely due to the axonal degeneration associated

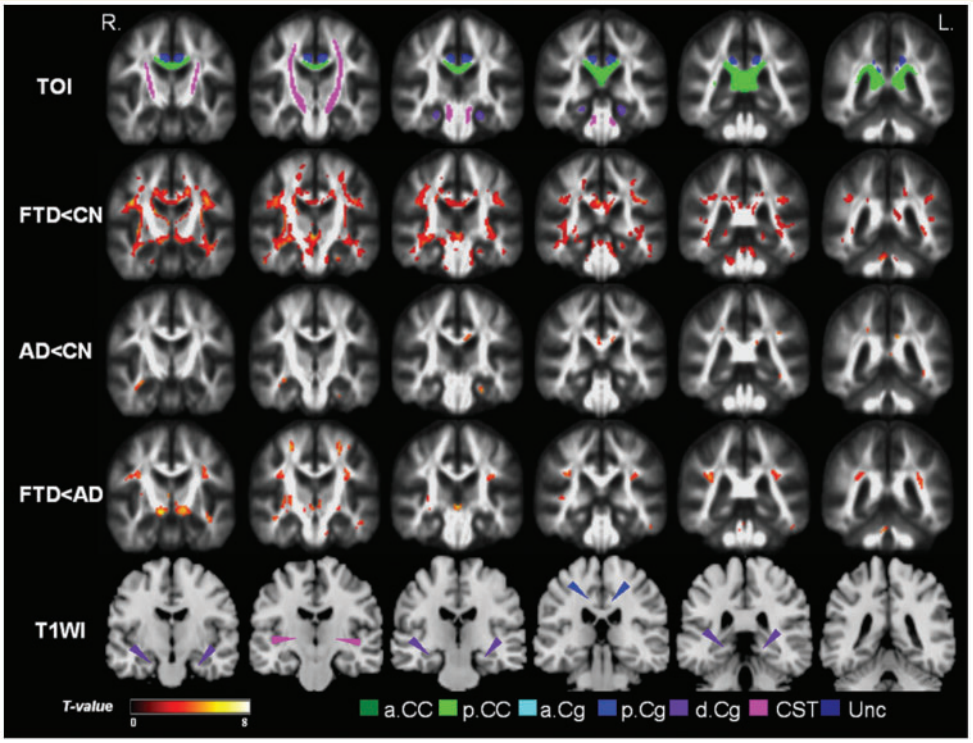

Figure 6 Coronal view of the regional FA reductions in the posterior brain comparing between groups: the top row indicates regions of the tracts of interest (TOIs) analysis for comparison with the voxel-wise analyses in the rows below. The second row (FTD<CN) shows FA reductions in FTD relative to cognitively normal involving the anterior frontal and temporal brain. FTD compared to cognitively normal had widely distributed changes involving the posterior brain (but not as strong as anterior brain) including posterior corpus callosum, bilateral posterior cingulum, descending cingulum fibres, as well as fibres in superior longitudinal fascicules. The third row (AD<CN) shows the regional FA reductions in Alzheimer's disease relative to cognitively normal involving a few regions in left posterior cingulum and left descending cingulum. The fourth row (FTD<AD) shows FA reductions in FTD relative to Alzheimer's disease indicating FTD had significantly lower FA in regions of the bilateral superior longitudinal fascicules and inferior thalamic areas. The last row (T1WI) depicts the anatomical locations on a T_1-weighted brain template. The areas with significantly decreased FA values are marked in warm colours with threshold $P_{FDR} = 0.05$.

with injury/death of grey matter neuronal cell bodies. However, these findings are also consistent with histopathological evidence of tau protein deposition in white matter of FTD (Schofield *et al*., 2003). Notably, we found substantial FA reduction in the bilateral descending cingulum, which is a major limbic fibre loop in the medial temporal lobe. The finding is consistent with reports from structural MRI studies of neurodegeneration of the paralimbic network in FTD (Rabinovici *et al*., 2007–08; Seeley *et al*., 2008), but has not been observed in DTI studies before.

Our findings of FA reductions in the parietal and temporal regions in Alzheimer's disease are in agreement with several other DTI studies (Takahashi *et al*., 2002; Fellgiebel *et al*., 2004; Naggara *et al*., 2006; Taoka *et al*., 2006; Xie *et al*., 2006; Stahl *et al*., 2007; Teipel *et al*., 2007; Salat *et al*., in press). DTI abnormalities in fibres located deep in the posterior white matter, such as the left posterior cingulum and the posterior corpus callosum have consistently been reported for Alzheimer's disease and even for mild cognitive impairment (MCI) (Fellgiebel *et al*., 2005; Medina *et al*., 2006; Stahl *et al*., 2007; Zhang *et al*., 2007; Parente *et al*., 2008), which is a diagnostic category that will include many subjects with a preclinical stage of Alzheimer's disease. In addition, we found abnormalities in the descending branch of cingulum (i.e. the parahippocampal fibre), consistent with histological, structural and metabolic studies suggesting that the medial temporal region is particularly vulnerable to Alzheimer's pathology (see review papers: Anderson *et al*., 2005; Drzezga, 2008; Ries *et al*., 2008). Moreover, the observation of FA reduction in the descending cingulum replicates our previous DTI results in an entirely different population of Alzheimer's disease and MCI patients (Zhang *et al*., 2007). More recently, altered diffusion properties of parahippocampal white matter in Alzheimer's disease were found even in absence of significant grey matter degeneration as measured by hippocampal atrophy (Salat *et al*., in press). These findings imply that disintegration of the parahippocampal fibres is a systematic and potentially early marker of incipient Alzheimer's disease. However, the pathological underpinning of FA changes in white matter in Alzheimer's disease remains elusive with several explanations possible. One possibility is that the degeneration of white matter is secondary to grey matter pathology. Alzheimer's disease is thought to begin in grey matter with deposition of β-amyloid around neuronal cell bodies. The disease is also associated with accumulation of tau protein in

neuronal cells (Hashimoto *et al*., 2003). These cellular processes lead to neurodegeneration including loss of axons within associated white matter tracks. This white matter degradation can then be detected via FA reductions measured by DTI. An alternative explanation is that white matter degeneration is a direct consequence of Alzheimer's pathology. Braak *et al*. (2000) hypothesized that as brain development takes place, regions that become myelinated later in the process, such as cortical association areas, have fewer oligodendrocytes supporting greater numbers of axons compared to regions that become myelinated earlier (primary sensorimotor regions). Oligodendrocytes have particularly high metabolic demands in the cortical association areas to maintain the distributed network of their axons, which makes these axons more susceptible to pathological processes such as oxidative stress (Bartzokis, 2004). These and other changes may lead to the diminished white matter integrity in the association cortical regions. Longitudinal studies, using DTI and cortical mapping together, are needed to investigate the relationship between white matter and grey matter changes in more detail.

Relative to Alzheimer's disease, FTD was associated with markedly reduced FA in the frontal brain regions. This finding is consistent with several structural and functional imaging studies which reported greater grey matter loss and reduced cerebral blood flow in frontal brain regions in FTD when compared to Alzheimer's disease (Julin *et al*., 1995; Kitagaki *et al*., 1998; Varma *et al*., 2002; Varrone *et al*., 2002). Taking these DTI, structural and functional findings in FTD together, the results emphasize an association between white matter degradation and cortical abnormalities in FTD. In contrast, Alzheimer's disease showed no significant FA reductions relative to FTD. This observation is surprising because several structural and functional imaging studies of Alzheimer's disease reported substantial abnormalities in posterior brain regions in Alzheimer's disease relative to FTD (Varrone *et al*., 2002; Du *et al*., 2006). One possible explanation is that white matter and grey matter are affected differently in Alzheimer's disease and FTD throughout the course of the disease. Our ongoing studies hope to better elucidate the relationship between grey matter and white matter changes in Alzheimer's disease and FTD. Another possibility, which cannot be ruled out is that the patients diagnosed with Alzheimer's disease in this study were at an earlier stage of the disease and less impaired than the FTD patients. It is difficult to compare disease severity in two different disorders which have quite different symptomatology. It is possible that these patients with Alzheimer's disease will eventually exhibit regions of reduced FA relative to FTD as the disease progresses. Prospective studies of FTD and Alzheimer's disease are needed to resolve this issue.

Examination of regional alterations in various diffusion parameters, including radial and D_{ax} in addition to anisotropy, showed distinct zones of alterations that potentially stemmed from different underlying pathological processes. For example, radial and D_{ax} of the uncinate fibres was substantially higher in FTD than in Alzheimer's disease where most regions of reduced FA values showed also increased D_{ra}. On the other hand, differences in diffusion anisotropy of the anterior corpus callosum fibres between FTD and Alzheimer's disease disappeared when analysed in terms of D_{ra}. These results suggest that some disease specificity may be obtained by further examination of different DTI eigenvalues. Diffusion studies in animals suggest that increased D_{ra} can be associated with myelin damage (Song *et al*., 2002; Harsan *et al*., 2006). Accordingly, our findings of increased D_{ra} in some regions in FTD and Alzheimer's disease, including the uncinate fibres, could reflect processes of demyelination. In contrast, demyelination would not explain the FA differences in anterior corpus callosum fibres between FTD and Alzheimer's disease, since D_{ra} was not significantly different. However, the interpretation of DTI indices with respect to pathology is notoriously ambiguous and more validation studies to the underlying causes of DTI changes are necessary.

Several limitations of our study ought to be mentioned. First, the clinical diagnoses were not confirmed by autopsy and, therefore, the pathological processes underlying the DTI alterations may not be associated with FTD and Alzheimer's disease. In particular, FTD, which is one of several variants of frontotemporal lobar degeneration that have different aetiologies, suffers from diagnostic uncertainty. Consequently, the pattern of DTI changes may vary among FTD patients with different aetiologies. Second, although the groups were matched for WMSH severity and regions including WMSH were avoided in analysis, WMSH due to cerebrovascular disease may have affected FA and the other DTI measures. The relation between fibre integrity and cerebrovascular disease needs to be explored further. Another concern is that large variations of brain shape in older subjects limited the ability to achieve spatial normalization of white matter regions across the subjects. This is particularly critical as cortical and ventricular shapes may have driven image registration. Some FA changes, especially in regions surrounding the ventricles as seen in Figs 5 and 6, could be a result of artefacts due to image misregistration and underlying variations of brain shapes. The use of more sophisticated algorithms for DTI registration such as Tract-Based Spatial Statistics (TBSS) (Smith *et al*., 2006) or dense feature deformation morphometry (Studholme, 2008) could lead to different results. Further studies involving a larger number of patients and autopsied confirmation of the pathology are needed to support our results.

In summary, the regional DTI alterations suggest that FTD and Alzheimer's disease are each associated with a characteristic distribution of white matter degradation. The results also suggest a greater vulnerability of white matter in FTD than in Alzheimer's disease. DTI may provide additional diagnostic information to distinguish Alzheimer's disease from FTD.

Acknowledgements

We thank Mr Christopher Ching and Mr Shannon Buckley for assistance with image processing and English editing.

Funding

National Institutes of Health grants (P01AG19724, P50 AG23501); Department of Defense (DAMD17-03-1-0532); Medical Research Service of the Department of Veterans Affairs (MIRECC).

References

Anderson VC, Litvack ZN, Kaye JA. Magnetic resonance approaches to brain aging and Alzheimer disease-associated neuropathology [Review]. Top Magn Reson Imaging 2005; 16: 439–52.

Aoki S, Iwata NK, Masutani Y, Yoshida M, Abe O, Ugawa Y, et al. Quantitative evaluation of the pyramidal tract segmented by diffusion tensor tractography: feasibility study to patients with amyotrophic lateral sclerosis. Radiat Med 2005; 23: 195–9.

Bartenstein P, Minoshima S, Hirsch C, Buch K, Willoch F, Mösch D, et al. Quantitative assessment of cerebral blood flow in patients with Alzheimer's disease by SPECT. J Nucl Med 1997; 38: 1095–101.

Bartzokis G. Age-related myelin breakdown: a developmental model of cognitive decline and Alzheimer's disease [Review]. Neurobiol Aging 2004; 25: 5–18.

Borroni B, Brambati SM, Agosti C, Gipponi S, Bellelli G, Gasparotti R, et al. Evidence of white matter changes on diffusion tensor imaging in frontotemporal dementia. Arch Neurol 2007; 64: 246–51.

Bozzali M, Falini A, Franceschi M, Cercignani M, Zuffi M, Scotti G, et al. White matter damage in Alzheimer's disease assessed in vivo using diffusion tensor magnetic resonance imaging. J Neurol Neurosurg Psychiatry 2002; 72: 742–6.

Braak H, Del Tredici K, Schultz C, Braak E. Vulnerability of select neuronal types to Alzheimer's disease. Ann N Y Acad Sci 2000; 924: 53–61.

Cardenas VA, Boxer AL, Chao LL, Gorno-Tempini ML, Miller BL, Weiner MW, et al. Deformation-based morphometry reveals brain atrophy in frontotemporal dementia. Arch Neurol 2007; 64: 873–7.

Chao LL, Schuff N, Clevenger EM, Mueller SG, Rosen HJ, Gorno-Tempini ML, et al. Patterns of white matter atrophy in frontotemporal lobar degeneration. Arch Neurol 2007; 64: 1619–24.

Charpentier P, Lavenu I, Defebvre L, Duhamel A, Lecouffe P, Pasquier F, et al. Alzheimer's disease and frontotemporal dementia are differentiated by discriminant analysis applied to (99m)Tc HmPAO SPECT data. J Neurol Neurosurg Psychiatry 2000; 69: 661–3.

Choi SJ, Lim KO, Monteiro I, Reisberg B. Diffusion tensor imaging of frontal white matter microstructure in early Alzheimer's disease: a preliminary study. J Geriatr Psychiatry Neurol 2005; 18: 12–9.

Coulthard E, Firbank M, English P, Welch J, Birchall D, O'Brien J, et al. Proton magnetic resonance spectroscopy in frontotemporal dementia. J Neurol 2006; 253: 861–8.

Diehl J, Grimmer T, Drzezga A, Riemenschneider M, Forstl H, Kurz A. Cerebral metabolic patterns at early stages of frontotemporal dementia and semantic dementia. A PET study. Neurobiol Aging 2004; 25: 1051–6.

Diehl-Schmid J, Grimmer T, Drzezga A, Bornschein S, Riemenschneider M, Förstl H, et al. Decline of cerebral glucose metabolism in frontotemporal dementia: a longitudinal 18F-FDG-PET-study. Neurobiol Aging 2007; 28: 42–50.

Double KL, Halliday GM, Kril JJ, Harasty JA, Cullen K, Brooks WS, et al. Topography of brain atrophy during normal aging and Alzheimer's disease. Neurobiol Aging 1996; 17: 513–21.

Drzezga A. Concept of functional imaging of memory decline in Alzheimer's disease [Review]. Methods 2008; 44: 304–14.

Du AT, Jahng GH, Hayasaka S, Kramer JH, Rosen HJ, Gorno-Tempini ML, et al. Hypoperfusion in frontotemporal dementia and Alzheimer disease by arterial spin labeling MRI. Neurology 2006; 67: 1215–20.

Ellis CM, Simmons A, Jones DK, Bland J, Dawson JM, Horsfield MA, et al. Diffusion tensor MRI assesses corticospinal tract damage in ALS. Neurology 1999; 53: 1051–8.

Fellgiebel A, Müller MJ, Wille P, Dellani PR, Scheurich A, Schmidt LG, et al. Color-coded diffusion-tensor-imaging of posterior cingulate fiber tracts in mild cognitive impairment. Neurobiol Aging 2005; 26: 1193–8.

Fellgiebel A, Wille P, Müller MJ, Winterer G, Scheurich A, Vucurevic G, et al. Ultrastructural hippocampal and white matter alterations in mild cognitive impairment: a diffusion tensor imaging study. Dement Geriatr Cogn Disord 2004; 18: 101–8.

Folstein MF, Folstein SE, McHugh PR. ''Mini-mental state'' A practical method for grading the cognitive state of patients for the clinician. J Psychiatr Res 1975; 12: 189–98.

Gee J, Ding L, Xie Z, Lin M, DeVita C, Grossman M. Alzheimer's disease and frontotemporal dementia exhibit distinct atrophy—behavior correlates: a computer-assisted imaging study. Acad Radiol 2003; 10: 1392–401.

Genovese CR, Lazar NA, Nichols T. Thresholding of statistical maps in functional neuroimaging using the false discovery rate. Neuroimage 2002; 15: 870–8.

Grimmer T, Diehl J, Drzezga A, Forstl H, Kurz A. Region-specific decline of cerebral glucose metabolism in patients with frontotemporal dementia: a prospective 18F-FDG-PET study. Dement Geriatr Cogn Disord 2004; 18: 32–6.

Griswold MA, Jakob PM, Heidemann RM, Nittka M, Jellus V, Wang J, et al. Generalized autocalibrating partially parallel acquisitions (GRAPPA). Magn Reson Med 2002; 47: 1202–10.

Harsan LA, Poulet P, Guignard B, Steibel J, Parizel N, de Sousa PL, et al. Brain dysmyelination and recovery assessment by noninvasive in vivo diffusion tensor magnetic resonance imaging. J Neurosci Res 2006; 83: 392–402.

Hashimoto M, Rockenstein E, Crews L, Masliah E. Role of protein aggregation in mitochondrial dysfunction and neurodegeneration in Alzheimer's and Parkinson's diseases. Neuromolecular Med 2003; 4: 21–36.

Head D, Buckner RL, Shimony JS, Williams LE, Akbudak E, Conturo TE, et al. Differential vulnerability of anterior white matter in nondemented aging with minimal acceleration in dementia of the Alzheimer type: evidence from diffusion tensor imaging. Cereb Cortex 2004; 4: 410–23.

Huang J, Friedland RP, Auchus AP. Diffusion tensor imaging of normal-appearing white matter in mild cognitive impairment and early Alzheimer disease: preliminary evidence of axonal degeneration in the temporal lobe. AJNR Am J Neuroradiol 2007; 28: 1943–8.

Ishii K, Sakamoto S, Sasaki M, Kitagaki H, Yamaji S, Hashimoto M, et al. Cerebral glucose metabolism in patients with frontotemporal dementia. J Nucl Med 1998; 39: 1875–8.

Jeong Y, Cho SS, Park JM, Kang SJ, Lee JS, Kang E, et al. 18F-FDG PET findings in frontotemporal dementia: an SPM analysis of 29 patients. J Nucl Med 2005; 46: 233–9.

Johnson KA, Mueller ST, Walshe TM, English RJ, Holman BL. Cerebral perfusion imaging in Alzheimer's disease. Use of single photon emission computed tomography and iofetamine hydrochloride I 123. Arch Neurol 1987; 44: 165–8.

Julin P, Wahlund LO, Basun H, Persson A, Mare K, Rudberg U. Clinical diagnosis of frontal lobe dementia and Alzheimer's disease: relation to cerebral perfusion, brain atrophy and electroencephalography. Dementia 1995; 6: 142–7.

Kim EJ, Cho SS, Jeong Y, Park KC, Kang SJ, Kang E, et al. Glucose metabolism in early onset versus late onset Alzheimer's disease: an SPM analysis of 120 patients. Brain 2005; 128: 1790–801.

Kitagaki H, Mori E, Yamaji S, Ishii K, Hirono N, Kobashi S, et al. Frontotemporal dementia and Alzheimer disease: evaluation of cortical atrophy with automated hemispheric surface display generated with MR images. Radiology 1998; 208: 431–9.

Laakso MP, Frisoni GB, Könönen M, Mikkonen M, Beltramello A, Geroldi C, et al. Hippocampus and entorhinal cortex in frontotemporal dementia and Alzheimer's disease: a morphometric MRI study. Biol Psychiatry 2000; 47: 1056–63.

Larsson E, Passant U, Sundgren PC, Englund E, Brun A, Lindgren A, et al. Magnetic resonance imaging and histopathology in dementia, clinically of frontotemporal type. Dement Geriatr Cogn Disord 2000; 11: 123–34.

Larsson EM, Englund E, Sjobeck M, Lätt J, Brockstedt S. MRI with diffusion tensor imaging post-mortem at 3.0 T in a patient with

frontotemporal dementia. Dement Geriatr Cogn Disord 2004; 17: 316–9.

Le Bihan D, Mangin JF, Poupon C, Clark CA, Pappata S, Molko N, et al. Diffusion tensor imaging: concepts and applications. J Magn Reson Imaging 2001; 13: 534–46.

Masutani Y, Aoki S, Abe O, Hayashi N, Otomo K. MR diffusion tensor imaging: recent advance and new techniques for diffusion tensor visualization. Eur J Radiol 2003; 46: 53–66.

Matsuo K, Mizuno T, Yamada K, Akazawa K, Kasai T, Kondo M, et al. Cerebral white matter damage in frontotemporal dementia assessed by diffusion tensor tractography. Neuroradiology 2008; 50: 605–11.

Medina D, DeToledo-Morrell L, Urresta F, Gabrieli JD, Moseley M, Fleischman D, et al. White matter changes in mild cognitive impairment and AD: a diffusion tensor imaging study. Neurobiol Aging 2006; 27: 663–72.

McKhann G, Drachman D, Folstein M, Katzman R, Price D, Stadlan EM. Clinical diagnosis of Alzheimer's disease: report of the NINCDSADRDA Work Group under the auspices of Department of Health and Human Services Task Force on Alzheimer's Disease. Neurology 1984; 34: 939–44.

McMurtray AM, Chen AK, Shapira JS, Chow TW, Mishkin F, Miller BL, et al. Variations in regional SPECT hypoperfusion and clinical features in frontotemporal dementia. Neurology 2006; 66: 517–22.

Miller BL, Cummings JL, Villanueva-Meyer J, Boone K, Mehringer CM, Lesser IM, et al. Frontal lobe degeneration: clinical, neuropsychological, and SPECT characteristics. Neurology 1991; 41: 1374–82.

Mori S, Crain BJ, Chacko VP, van Zijl PCM. Three-dimensional tracking of axonal projections in the brain by magnetic resonance imaging. Ann Neurol 1999; 45: 265–9.

Morris JC. The clinical dementia rating (CDR): current version and scoring rules. Neurology 1993; 43: 2412–4.

Naggara O, Oppenheim C, Rieu D, Raoux N, Rodrigo S, Dalla Barba G, et al. Diffusion tensor imaging in early Alzheimer's disease. Psychiatry Res 2006; 146: 243–9.

Neary D, Snowden JS, Gustafson L, Passant U, Stuss D, Black S, et al. Frontotemporal lobar degeneration: a consensus on clinical diagnostic criteria. Neurology 1998; 51: 1546–54.

Parente DB, Gasparetto EL, da Cruz LC Jr, Domingues RC, Baptista AC, Carvalho AC, et al. Potential role of diffusion tensor MRI in the differential diagnosis of mild cognitive impairment and Alzheimer's disease. AJR Am J Roentgenol 2008; 190: 1369–74.

Perry RJ, Graham A, Williams G, Rosen H, Erzinçlioglu S, Weiner M, et al. Patterns of frontal lobe atrophy in frontotemporal dementia: a volumetric MRI study. Dement Geriatr Cogn Disord 2006; 22: 278–87.

Pickut BA, Saerens J, Mariën P, Borggreve F, Goeman J, Vandevivere J, et al. Discriminative use of SPECT in frontal lobe-type dementia versus (senile) dementia of the Alzheimer's type. J Nucl Med 1997; 38: 929–34.

Pierpaoli C, Basser PJ. Toward a quantitative assessment of diffusion anisotropy. Magn Reson Med 1996; 36: 893–906.

Rabinovici GD, Seeley WW, Kim EJ, Gorno-Tempini ML, Rascovsky K, Pagliaro TA, et al. Distinct MRI atrophy patterns in autopsy-proven Alzheimer's disease and frontotemporal lobar degeneration. Am J Alzheimers Dis Other Demen 2007–2008; 22: 474–88.

Ries ML, Carlsson CM, Rowley HA, Sager MA, Gleason CE, Asthana S, et al. Magnetic resonance imaging characterization of brain structure and function in mild cognitive impairment: a review. J Am Geriatr Soc 2008; 56: 920–34.

Ringman JM, O'Neill J, Geschwind D, Medina L, Apostolova LG, Rodriguez Y, et al. Diffusion tensor imaging in preclinical and presymptomatic carriers of familial Alzheimer's disease mutations. Brain 2007; 130: 1767–76.

Rose SE, Chen F, Chalk JB, Zelaya FO, Strugnell WE, Benson M, et al. Loss of connectivity in Alzheimer's disease: an evaluation of white matter tract integrity with colour coded MR diffusion tensor imaging. J Neurol Neurosurg Psychiatry 2000; 69: 528–30.

Rose SE, Janke AL, Chalk JB. Gray and white matter changes in Alzheimer's disease: a diffusion tensor imaging study. J Magn Reson Imaging 2008; 27: 20–6.

Rosen HJ, Gorno-Tempini ML, Goldman WP, Perry RJ, Schuff N, Weiner M, et al. Patterns of brain atrophy in frontotemporal dementia and semantic dementia. Neurology 2002; 58: 198–208.

Salat DH, Tuch DS, van der Kouwe AJ, Greve DN, Pappu V, Lee SY, *et al*., White matter pathology isolates the hippocampal formation in Alzheimer's disease. Neurobiol Aging in press.

Scheltens P, Barkhof F, Leys D, Pruvo JP, Nauta JJ, Vermersch P, et al. Semiquantative rating scale for the assessment of signal hyperintensities on magnetic resonance imaging. J Neurol Sci 1993; 114: 7–12.

Schofield E, Kersaitis C, Shepherd CE, Kril JJ, Halliday GM. Severity of gliosis in Pick's disease and frontotemporal lobar degeneration: tau-positive glia differentiate these disorders. Brain 2003; 126: 827–40.

Seeley WW, Crawford R, Rascovsky K, Kramer JH, Weiner M, Miller BL, et al. Frontal paralimbic network atrophy in very mild behavioral variant frontotemporal dementia. Arch Neurol 2008; 65: 249–55.

Shiga K, Yamada K, Yoshikawa K, Mizuno T, Nishimura T, Nakagawa M. Local tissue anisotropy decreases in cerebellopetal fibers and pyramidal tract in multiple system atrophy. J Neurol 2005; 252: 589–96.

Siri S, Benaglio I, Frigerio A, Binetti G, Cappa SF. A brief neuropsychological assessment for the differential diagnosis between frontotemporal dementia and Alzheimer's disease. Eur J Neurol 2001; 8: 125–32.

Smith SM, Jenkinson M, Johansen-Berg H, Rueckert D, Nichols TE, Mackay CE, et al. Tract-based spatial statistics: voxelwise analysis of multi-subject diffusion data. Neuroimage 2006; 31: 1487–505.

Song SK, Sun SW, Ramsbottom MJ, Chang C, Russell J, Cross AH. Dysmyelination revealed through MRI as increased radial (but unchanged axial) diffusion of water. Neuroimage 2002; 17: 1429–36.

Stahl R, Dietrich O, Teipel SJ, Hampel H, Reiser MF, Schoenberg SO. White matter damage in Alzheimer disease and mild cognitive impairment: assessment with diffusion-tensor MR imaging and parallel imaging techniques. Radiology 2007; 243: 483–92.

Studholme C. Dense feature deformation morphometry: incorporating DTI data into conventional MRI morphometry. Med Image Anal 2008; 12: 742–51.

Sugihara S, Kinoshita T, Matsusue E, Fujii S, Ogawa T. Usefulness of diffusion tensor imaging of white matter in Alzheimer disease and vascular dementia. Acta Radiol 2004; 45: 658–63.

Takahashi S, Yonezawa H, Takahashi J, Kudo M, Inoue T, Tohgi H. Selective reduction of diffusion anisotropy in white matter of Alzheimer disease brains measured by 3.0 Tesla magnetic resonance imaging. Neurosci Lett 2002; 332: 45–8.

Taoka T, Iwasaki S, Sakamoto M, Nakagawa H, Fukusumi A, Myochin K, et al. Diffusion anisotropy and diffusivity of white matter tracts within the temporal stem in Alzheimer disease: evaluation of the 'tract of interest' by diffusion tensor tractography. AJNR Am J Neuroradiol 2006; 27: 1040–5.

Teipel SJ, Bayer W, Alexander GE, Zebuhr Y, Teichberg D, Kulic L, et al. Progression of corpus callosum atrophy in Alzheimer disease. Arch Neurol 2002; 59: 243–8.

Teipel SJ, Stahl R, Dietrich O, Schoenberg SO, Perneczky R, Bokde AL, et al. Multivariate network analysis of fiber tract integrity in Alzheimer's disease. Neuroimage 2007; 34: 985–95.

Varma AR, Adams W, Lloyd JJ, Carson KJ, Snowden JS, Testa HJ, et al. Diagnostic patterns of regional atrophy on MRI and regional cerebral blood flow change on SPECT in young onset patients with Alzheimer's disease, frontotemporal dementia and vascular dementia. Acta Neurol Scand 2002; 105: 261–9.

Varrone A, Pappatà S, Caracò C, Soricelli A, Milan G, Quarantelli M, et al. Voxel-based comparison of rCBF SPET images in frontotemporal dementia and Alzheimer's disease highlights the involvement of

different cortical networks. Eur J Nucl Med Mol Imag 2002; 29: 1447–54.

Wakana S, Jiang H, Nagae-Poetscher LM, van Zijl PC, Mori S. Fiber tract-based atlas of human white matter anatomy. Radiology 2004; 230: 77–87.

Whitwell JL, Jack CR Jr, Senjem ML, Josephs KA. Patterns of atrophy in pathologically confirmed FTLD with and without motor neuron degeneration. Neurology 2006; 66: 102–4.

Xie S, Xiao JX, Gong GL, Zang YF, Wang YH, Wu HK, et al. Voxel-based detection of white matter abnormalities in mild Alzheimer disease. Neurology 2006; 66: 1845–9.

Yasmin H, Nakata Y, Aoki S, Abe O, Sato N, Nemoto K, et al. Diffusion abnormalities of the uncinate fasciculus in Alzheimer's disease: diffusion tensor tract-specific analysis using a new method to measure the core of the tract. Neuroradiology 2008; 50: 293–9.

Yoshikawa K, Nakata Y, Yamada K, Nakagawa M. Early pathological changes in the parkinsonian brain demonstrated by diffusion tensor MRI. J Neurol Neurosurg Psychiatry 2004; 75: 481–4.

Zhang Y, Schuff N, Jahng GH, Bayne W, Mori S, Schad L, et al. Diffusion tensor imaging of cingulum fibers in mild cognitive impairment and Alzheimer disease. Neurology 2007; 68: 13–9.